

## Supporting Information

### Near-Unity Photoluminescence Quantum Yield in Zero-Dimensional Lead-free Indium-Based Hybrid Perovskites by Antimony Doping

Jingheng Nie<sup>‡, 1</sup>, Xiangyan Yun<sup>‡, 2</sup>, Fangrui Cheng<sup>1</sup>, Ban Lan<sup>1, \*</sup>, Renping Cao<sup>1, \*</sup>, Jing Wang<sup>1, 3, \*</sup>

<sup>1</sup> *Guangdong Rare Earth Photofunctional Materials Engineering Technology Research Center, School of Chemistry and Environment, Jiaying University, Meizhou, 514015, P. R. China*

<sup>2</sup> *International Collaborative Laboratory of 2D Materials for Optoelectronics Science and Technology of Ministry of Education, Institute of Microscale Optoelectronics, Shenzhen University, Shenzhen 518060, P. R. China*

<sup>3</sup> *Ministry of Education Key Laboratory of Bioinorganic and Synthetic Chemistry, State Key Laboratory of Optoelectronic Materials and Technologies, Sun Yat-Sen University, Guangzhou, Guangdong 510275, China*

\*R. C. E-mail: jxcrp@163.com

\*B. L. E-mail: jyulb6@163.com

\*J. W. E-mail: ceswj@mail.sysu.edu.cn

‡ The authors contributed equally to this work.

## **Experimental section**

### **1. Materials:**

Indium(III) chloride ( $\text{InCl}_3$ , 99.99% metal basis) and *N,N*-Dimethylformamide ( $\text{C}_3\text{H}_7\text{NO}$ , DMF) were purchased from Macklin. Antimony trichloride ( $\text{SbCl}_3$ , 99.9% metal basis) was purchased from Aladdin. Tetramethylammonium chloride ( $\text{C}_4\text{H}_{12}\text{NCl}$ , TMAC, 98% metals basis) was purchased from Shanghai Acmec Biochemical Co., Ltd., China. Hydrochloric acid ( $\text{HCl}$ , 38% in water by weight) was purchased from Sinopharm Chemical Reagent Co. Ltd., China. All chemicals were used as received without further purification.

### **2. Preparation of Single Crystals and LEDs:**

#### **2.1 Growth of $(\text{C}_4\text{H}_{12}\text{N})_2\text{InCl}_5 \cdot \text{DMF}$ and $(\text{C}_4\text{H}_{12}\text{N})_2\text{InCl}_5 \cdot \text{DMF}:\text{Sb}^{3+}$ Single Crystals.**

First,  $\text{InCl}_3$  (2 mmol, 4424 g) and TMAC (4 mmol, 0.4384 g) were dissolved in 8 mL of DMF solution. Then transfer it to a Teflon autoclave and add 2 mL of HCl. The mixture was heated at 175°C for 12 h and slowly cooled to 30°C. The transparent bulk crystals were synthesized, washed with DMF, and dried in a vacuum oven at 65°C overnight. Similarly, to obtain the  $\text{Sb}^{3+}$ -doped crystals, varying amounts of  $\text{SbCl}_3$  were added to the Teflon autoclave, when the total amount of  $\text{SbCl}_3$  and  $\text{InCl}_3$  is 2 mmol.

#### **2.2 Fabrication of LEDs**

This work thoroughly stirred the mixture of  $(\text{C}_4\text{H}_{12}\text{N})_2\text{InCl}_5 \cdot \text{DMF}:\text{Sb}^{3+}$  samples and epoxy resin AB adhesive, and coated the prepared mixture on the LED chip (310 nm), followed by drying treatment.

### **3. Characterization:**

The powder XRD (PXRD) patterns were performed by grinding  $(C_4H_{12}N)_2InCl_5 \cdot DMF$  crystals into fine powders in a mortar, using an X-ray diffractometer (D2 Phaser) with Cu K $\alpha$  radiation at  $\lambda = 1.5418 \text{ \AA}$ . The single-crystal XRD (SCXRD) pattern was measured using SuperNova single crystal diffractometer (EosS2 diffractometer). A simulation PXRD data was obtained by single-crystal XRD. UV-vis absorption spectra were recorded on a domestically produced ultraviolet spectrophotometer (UV-2600i, Shimadzu). The PLE spectra, the PL spectra, and the decay curves were measured using an Edinburgh fluorescence spectrophotometer (FS5). PLQYs were measured using a FS5 fluorescence spectrometer with an integrating sphere attachment. The excitation and emitted light from all directions of the sample surface were homogenized by the integrating sphere, and light at the exit port entered the monochromator to be detected. The specific PLQY calculation formula is as follows:

$$\Phi = \frac{E_c - E_a}{L_a - L_c}$$

where  $\Phi$  is the absolute PLQY,  $L_a$  is the total amount of excitation light,  $L_c$  is the amount of residual excitation light after direct excitation,  $E_c$  is the amount of emitted light, and  $E_a$  is the sphere's background. Spectral correction (emission arm) is applied to the raw data after background subtraction, and from these spectrally corrected curves the quantum yield is calculated using aF900 software wizard.

The PL spectra of LEDs were measured by a handheld spectroradiometer (HPCS320D, HOPOOCOLOR).



**Table S1.** Crystal data and structure refinement for  $(\text{C}_4\text{H}_{12}\text{N})_2\text{InCl}_5 \cdot \text{DMF}$  at 293.15 K.

Empirical formula	$\text{C}_{11}\text{H}_{31}\text{Cl}_5\text{InN}_3\text{O}$
Formula weight	457.24
Temperature/K	513.46
Crystal system	Monoclinic
Space group	$\text{C}2/\text{c}$
a/ $\text{\AA}$	13.7556(18)
b/ $\text{\AA}$	11.5098(11)
c/ $\text{\AA}$	13.7448(17)
$\alpha/^\circ$	90
$\beta/^\circ$	94.594(11)
$\gamma/^\circ$	90
Volume/ $\text{\AA}^3$	2169.1(4)
Z	4
$\rho_{\text{calcg}}/\text{cm}^3$	1.572
$\mu/\text{mm}^{-1}$	1.707
F(000)	1040.0
Radiation	MoK $\alpha$ ( $\lambda = 0.71073$ )
2 $\theta$ range for data collection/ $^\circ$	7.08 to 49.964
Index ranges	$-16 \leq h \leq 16, -13 \leq k \leq 13, -16 \leq l \leq 15$
Reflections collected	9555
Independent reflections	1906 [ $R_{\text{int}} = 0.2292, R_{\text{sigma}} = 0.1016$ ]
Data/restraints/parameters	1906/18/112
Goodness-of-fit on F <sup>2</sup>	1.065
Final R indexes [I $\geq 2\sigma$ (I)]	$R_1 = 0.0891, wR_2 = 0.2277$
Final R indexes [all data]	$R_1 = 0.0952, wR_2 = 0.2362$
Largest diff. peak/hole / e $\text{\AA}^{-3}$	2.29/-1.50

**Table S2.** Fractional Atomic Coordinates ( $\times 10^4$ ) and Equivalent Isotropic Displacement Parameters ( $\text{\AA}^2 \times 10^3$ ) for  $(\text{C}_4\text{H}_{12}\text{N})_2\text{InCl}_5 \cdot \text{DMF}$  at 293.15 K.  $U_{\text{eq}}$  is defined as 1/3 of the trace of the orthogonalized  $U_{\text{IJ}}$  tensor.

Atom	<i>x</i>	<i>y</i>	<i>z</i>	$U_{\text{eq}}$
In1	5000	2638.6(7)	7500	33.7(5)
Cl1	5393.6(17)	2842(3)	9281.1(15)	56.1(8)
Cl2	3224.8(19)	2749(3)	7785(2)	67.0(9)
Cl3	5000	495(3)	7500	53.5(9)
O1	5235(9)	4613(11)	7315(10)	52(3)
N1	5000	6467(9)	7500	47(2)
C2	4484(12)	7130(15)	8140(12)	99(4)
C1	4846(12)	5342(15)	7767(12)	46(4)
N2	2755	-109(6)	4960(4)	39.5(15)
C3	2520(8)	659(10)	5767(7)	65(3)
C4	3119(10)	604(12)	4170(8)	82(4)
C5	3528(9)	-961(11)	5304(9)	77(3)
C6	1866(8)	-746(11)	4590(10)	76(3)

**Table S3.** Anisotropic Displacement Parameters ( $\text{\AA}^2 \times 10^3$ ) for  $(\text{C}_4\text{H}_{12}\text{N})_2\text{InCl}_5 \cdot \text{DMF}$ .  
 The Anisotropic displacement factor exponent takes the form:  $-2\pi^2 [h^2a^{*2}U_{11} + 2hka^{*b*}U_{12} + \dots]$ .

Atom	U <sub>11</sub>	U <sub>22</sub>	U <sub>33</sub>	U <sub>23</sub>	U <sub>13</sub>	U <sub>12</sub>
In1	44.3(7)	31.4(7)	23.1(7)	0	-11.5(4)	0
Cl1	58.2(14)	83.9(18)	23.2(12)	-11.9(11)	-13.9(9)	-0.5(12)
Cl2	50.0(14)	107(2)	41.6(15)	-8.2(13)	-8.8(11)	24.6(13)
Cl3	65.3(19)	30.6(15)	62(2)	0	-8.4(15)	0
O1	55(5)	47(5)	55(5)	1(4)	9(4)	-1(4)
N1	68(6)	36(6)	35(5)	0	-18(4)	0
C2	105(8)	116(8)	81(7)	-8(7)	37(6)	-13(7)
C1	48(5)	45(5)	45(6)	0(4)	5(4)	-2(4)
N2	51(3)	39(3)	27(3)	2(3)	-3(3)	1(3)
C3	70(6)	69(6)	55(6)	-15(5)	2(5)	6(5)
C4	116(9)	80(8)	52(6)	18(6)	22(6)	-11(7)
C5	81(7)	78(8)	69(7)	-4(6)	-17(6)	31(6)
C6	66(6)	76(8)	83(8)	-9(7)	-15(6)	-18(6)

**Table S4.** Bond Lengths for  $(C_4H_{12}N)_2InCl_5 \cdot DMF$  at 293.15 K.

Atom	Atom	Length/ $\text{\AA}$	Atom	Atom	Length/ $\text{\AA}$
In1	Cl1	2.476(2)	N1	C2 <sup>1</sup>	1.400(15)
In1	Cl1 <sup>1</sup>	2.476(2)	N1	C2	1.400(15)
In1	Cl2	2.507(3)	N1	C1	1.367(19)
In1	Cl2 <sup>1</sup>	2.507(3)	N2	C3	1.474(11)
In1	Cl3	2.467(3)	N2	C4	1.479(11)
In1	O1	2.313(13)	N2	C5	1.495(12)
O1	C1	1.195(17)	N2	C6	1.480(12)

**Table S5.** Bond Angles for  $(C_4H_{12}N)_2InCl_5 \cdot DMF$  at 293.15 K.

Atom	Atom	Atom	Angle/ $^\circ$	Atom	Atom	Atom	Angle/ $^\circ$
Cl1 <sup>1</sup>	In1	Cl1	169.16(14)	O1	In1	Cl2 <sup>1</sup>	77.7(3)
Cl1 <sup>1</sup>	In1	Cl2 <sup>1</sup>	88.82(9)	O1	In1	Cl3	169.4(3)
Cl1	In1	Cl2 <sup>1</sup>	90.63(9)	C1	O1	In1	124.1(9)
Cl1	In1	Cl2	88.82(9)	C2	N1	C2 <sup>1</sup>	114.0(15) )
Cl1 <sup>1</sup>	In1	Cl2	90.63(9)	C1	N1	C2 <sup>1</sup>	141.4(11) )
Cl2	In1	Cl2 <sup>1</sup>	174.19(15)	C1	N1	C2	104.5(9)
Cl3	In1	Cl1 <sup>1</sup>	95.42(7)	O1	C1	N1	116.1(12) )
Cl3	In1	Cl1	95.42(7)	C3	N2	C4	109.1(9)
Cl3	In1	Cl2	92.90(8)	C3	N2	C5	110.3(7)
Cl3	In1	Cl2 <sup>1</sup>	92.91(8)	C3	N2	C6	109.3(8)
O1	In1	Cl1	89.7(4)	C4	N2	C5	108.8(9)
O1	In1	Cl1 <sup>1</sup>	79.6(4)	C4	N2	C6	110.0(8)
O1	In1	Cl2	96.5(3)	C6	N2	C5	109.3(9)

**Table S6.** Torsion Angles for  $(\text{C}_4\text{H}_{12}\text{N})_2\text{InCl}_5 \cdot \text{DMF}$  at 293.15 K.

A	B	C	D	Angle/ $^\circ$
In1	O1	C1	N1	-174.2(10)
C2	N1	C1	O1	-179.2(15)
C2 <sup>1</sup>	N1	C1	O1	-3(3)

**Table S7.** Hydrogen Atom Coordinates ( $\text{\AA} \times 10^4$ ) and Isotropic Displacement Parameters ( $\text{\AA}^2 \times 10^3$ ) for  $(\text{C}_4\text{H}_{12}\text{N})_2\text{InCl}_5 \cdot \text{DMF}$  at 293.15 K.

Atom	x	y	z	U <sub>eq</sub>
H2A	4792.9	7873.36	8238.98	149
H2B	4479.06	6733.75	8754.34	149
H2C	3825.98	7237.69	7866.32	149
H1	4460.89	5154.64	8270.46	55
H3A	3061.87	1164.1	5936.5	97
H3B	2389.08	196.45	6322.84	97
H3C	1954.69	1115.26	5566.14	97
H4A	2636.01	1170.8	3957.67	123
H4B	3249.38	112.13	3631.94	123
H4C	3708.41	991.6	4409.56	123
H5A	4063.18	-554.89	5642.84	116
H5B	3753.41	-1363.59	4753.85	116
H5C	3263.79	-1509.93	5737.98	116
H6A	1480.98	-922.51	5123.01	114
H6B	1480.98	-1455.57	4285.08	114
H6C	1492.39	-274.48	4120.8	114

**Table S8.** Atomic Occupancy for  $(\text{C}_4\text{H}_{12}\text{N})_2\text{InCl}_5 \cdot \text{DMF}$  at 293.15 K.

Atom	Occupancy
O1	0.5
C1	0.5
H1	0.5

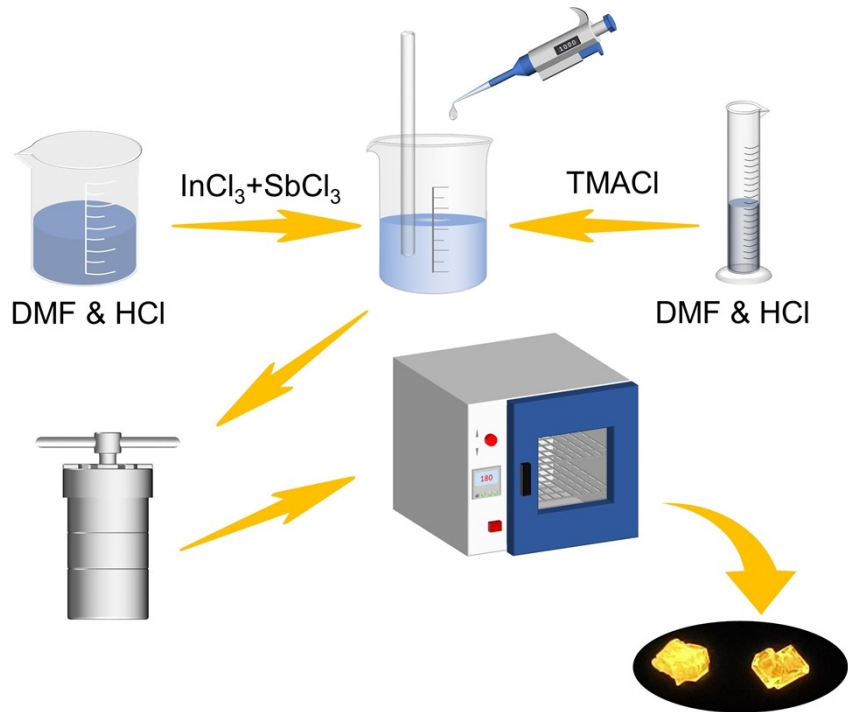


**Figure S1.** Schematic diagram of the preparation of  $(\text{C}_4\text{H}_{12}\text{N})_2\text{InCl}_5 \cdot \text{DMF}$  and  $(\text{C}_4\text{H}_{12}\text{N})_2\text{InCl}_5 \cdot \text{DMF}:\text{Sb}^{3+}$  single crystals via facile solution processing.

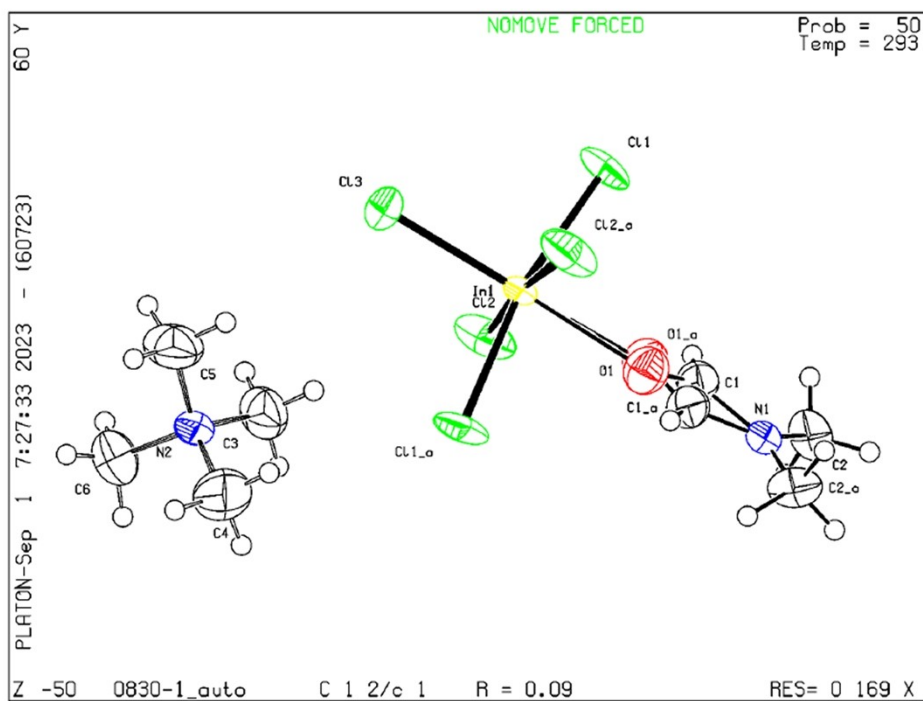


**Figure S2.** Oak Ridge thermal ellipsoid plot (ORTEP) for  $(\text{C}_4\text{H}_{12}\text{N})_2\text{InCl}_5 \cdot \text{DMF}$ .

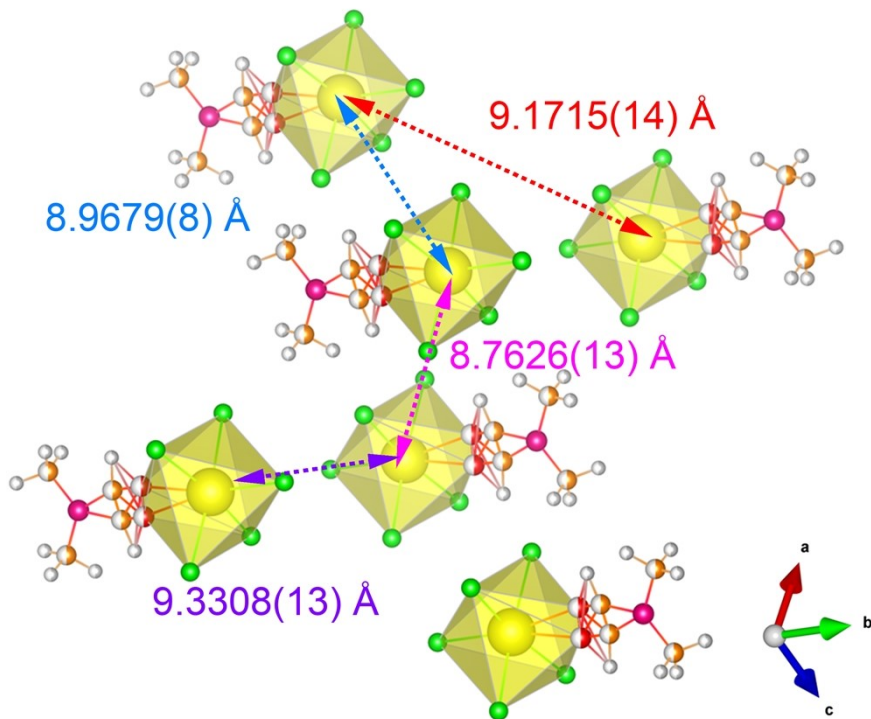


**Figure S3.** Crystal structure features of  $(\text{C}_4\text{H}_{12}\text{N})_2\text{InCl}_5 \cdot \text{DMF}$ .

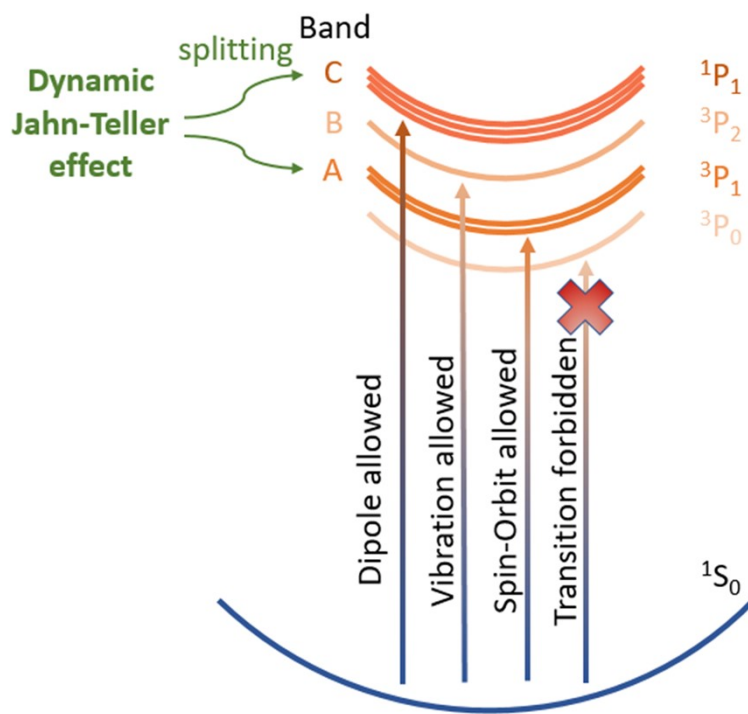


**Figure S4.** Schematic of the excitation process and excitation state of  $\text{Sb}^{3+}$  in metal halides.

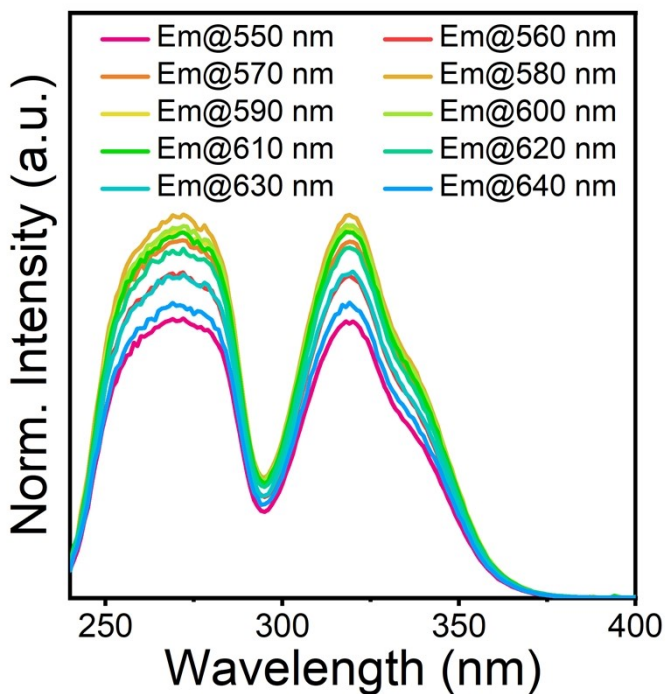


**Figure S5.** PLE curves of  $(\text{C}_4\text{H}_{12}\text{N})_2\text{InCl}_5 \cdot \text{DMF}:\text{Sb}^{3+}$  monitored at different emission wavelengths.

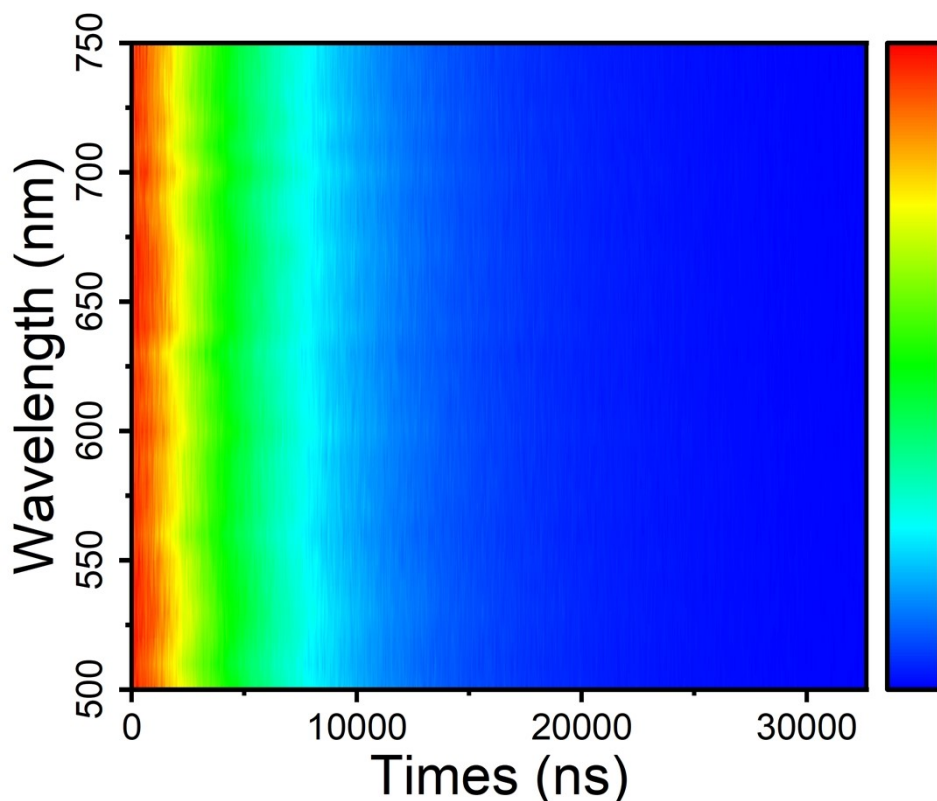


**Figure S6.** Emission wavelength scanning decay of  $(\text{C}_4\text{H}_{12}\text{N})_2\text{InCl}_5 \cdot \text{DMF}:\text{Sb}^{3+}$  excited by 320 nm.

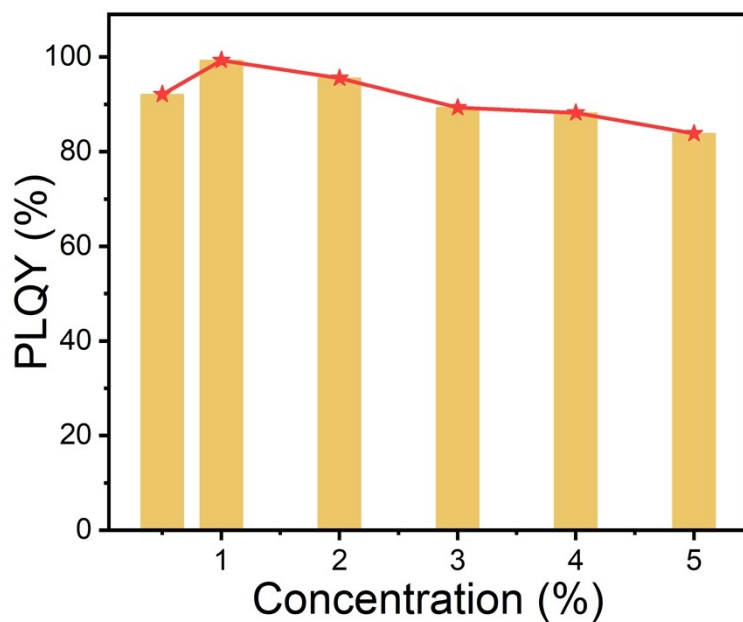


**Figure S7.** PLQY data for  $(C_4H_{12}N)_2InCl_5 \cdot DMF : xSb^{3+}$  samples at RT.

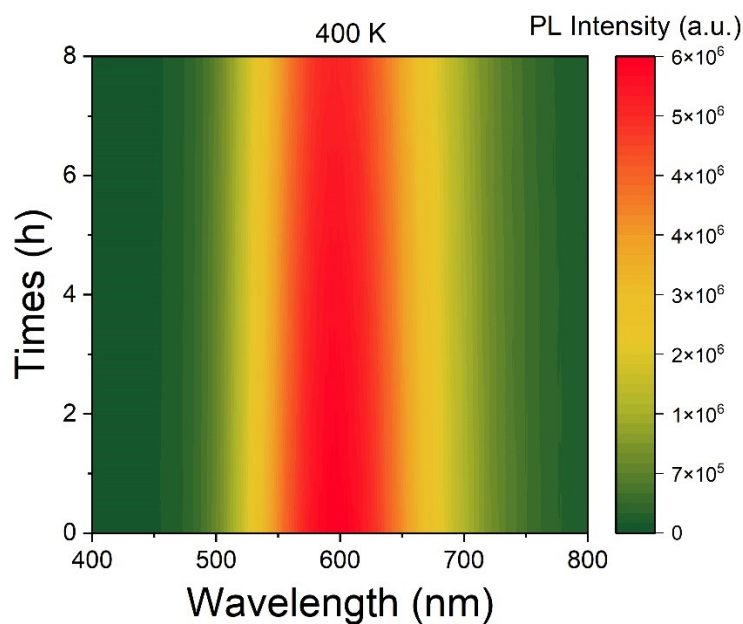


**Figure S8.** The PL-temperature correlation map of  $(C_4H_{12}N)_2InCl_5 \cdot DMF : Sb^{3+}$  maintained at 400 K for 8 h.